J. Mech. Phys. Solids 193 (2024) 105858

Contents lists available at ScienceDirect

Journal of the Mechanics and Physics of Solids

journal homepage: www.elsevier.com/locate/jmps

Adhesive and cohesive fracture of blood clots: Experiments and modeling

Shiyu Liu [a], Aram Bahmani [a], Gabriella Paige Sugerman [b], Zhen Yang [a], Manuel Rausch [b], Farshid Ghezelbash [a,*], Jianyu Li [a,c,*]

[a] Department of Mechanical Engineering, McGill University, Montreal, Canada
[b] Department of Aerospace Engineering & Engineering Mechanics, University of Texas at Austin, United States
[c] Department of Biomedical Engineering, McGill University, Montreal, Canada

ARTICLE INFO

Keywords:
Adhesion
Fracture
Cohesive zone model
Blood clots
RBC
Platelet

ABSTRACT

Blood clots represent living materials composed of a polymer network and an abundance of cells. They might fracture within the bulk material of the clot (cohesive fracture), at the interface between the clot and the surrounding tissue (adhesive fracture), or through a combination of both modes (hybrid fracture). The clot fracture within vascular systems and injury sites could lead to life-threatening conditions. Despite the significance, understanding and modeling the fracture behaviors of blood clots, including their dependence on mechanical loading and cellular components, remain in a nascent stage. In this study, we employ an integrated experimental-computational approach to comprehensively investigate the fracture behaviors of bovine blood clots. We explore various mechanical factors, substrates, and cellular components such as red blood cells (RBCs) and platelets. Our findings reveal that among various tissue substrates, blood clots exhibit the highest interfacial adhesion energy with muscle, and the lowest to the inner arterial lining, consistent with their biological function. Both interfacial adhesion energy and bulk fracture energy are rate-dependent, although they exhibit different dependencies. Also, RBCs and platelets have different effects on clot fracture. An increase in RBC content tends to toughen both adhesion and fracture of blood clots. However, an increase in platelet content enhances interfacial adhesion energy but lowers the bulk fracture energy. The platelet content also governs the shift from adhesive fracture to hybrid fracture. To model clot fracture, we developed two finite element models incorporating a coupled cohesive-zone and Mullins-effect approach to simulate pure shear fracture and peeling of blood clots. These models, validated through experimental data, elucidate the interplay between intrinsic fracture toughness, interfacial strength, and bulk energy dissipation during clot fracture. This study significantly advances our understanding of clot mechanics, providing valuable insights into the mechanics of similar living materials and the management of clot-related disorders such as hemorrhage and thrombosis.

1. Introduction

Blood clots are aggregates of fibrin fibers and blood cells. They could form at injury sites to halt bleeding or within blood vessels,

* Corresponding authors.
E-mail addresses: farshid.ghezelbash@mail.mcgill.ca (F. Ghezelbash), jianyu.li@mcgill.ca (J. Li).

https://doi.org/10.1016/j.jmps.2024.105858
Received 18 May 2024; Received in revised form 7 August 2024; Accepted 7 September 2024
Available online 10 September 2024

where they can block blood flow. Blood clots play a critical role in hemostasis and thrombosis (Jiang et al., 2022; Tanaka et al., 2009), and also find significant usage for tissue repair and regeneration (Bayer, 2022; Brown and Barker, 2014; Laurens et al., 2006). Clinical evidence underscores the importance of blood clot fracture: at bleeding sites, clot fracture leads to re-bleeding and potentially fatal hemorrhage; within blood vessels, fragments of fractured clots can migrate through the blood circulatory system, causing deep vein thrombosis and stroke. These complications could be further exacerbated by conditions such as blood disorders and COVID-19 (Ackermann et al., 2020). Blood clot fracture also limits their performance and application in biomedical fields, such as endovascular embolization surgery and regenerative medicine. Whereas the biochemical aspects of blood clots and clotting have been extensively studied, research on blood clot fracture remains in an early stage (Fereidoonnezhad et al., 2021; Liu et al., 2021; Tutwiler et al., 2020).

Due to their unique structure and composition, blood clots differ from other material systems such as hydrogels. While containing a fibrin network, they comprise a large volume fraction of biological cells such as red blood cells and platelets, which provide various biological and mechanical functions, such as binding with biological tissues and active contraction (Lam et al., 2011; Litvinov and Weisel, 2022; Qiu et al., 2019; Sugerman et al., 2020). These constituents could change with various disorders or conditions, such as polycythemia leading to high RBC count, and thrombocytopenia causing low platelet count. Exploring the role of biological cells is crucial for uncovering the underlying mechanisms of clot fracture with clinical implications (Ghezelbash et al., 2022; Liu et al., 2024). While the influence of fibrin content on cohesive fracture has been evaluated (Fereidoonnezhad et al., 2021), the effects of RBCs and platelets on clot fracture are less explored, and broadly the mechanical contributions of biological cells to the macroscopic fracture of soft materials remain elusive (Jiang et al., 2018). Investigating the mechanical behaviors of blood clots will greatly expand our knowledge of the mechanics of soft and living materials.

Recent years witnessed a surge of interest in clot fracture. Research efforts have been centered around cohesive fracture arising from crack propagation within the bulk matrix of clots (Fereidoonnezhad et al., 2021; Liu et al., 2021; Tutwiler et al., 2020). While clots often interface with biological tissues, another failure mode, adhesive fracture, resulting from the progression of an interfacial crack between the clot and a substrate tissue is equally important but less explored (Fig. 1) (Chan et al., 2020). The adhesive fracture of clots has been linked with rebleeding in animal experiments (Chan et al., 2020), as well as the fragmentation of thrombi in blood vessels. Moreover, crack propagation at the clot-tissue interface could proceed partly along the interface (adhesive) and partly within

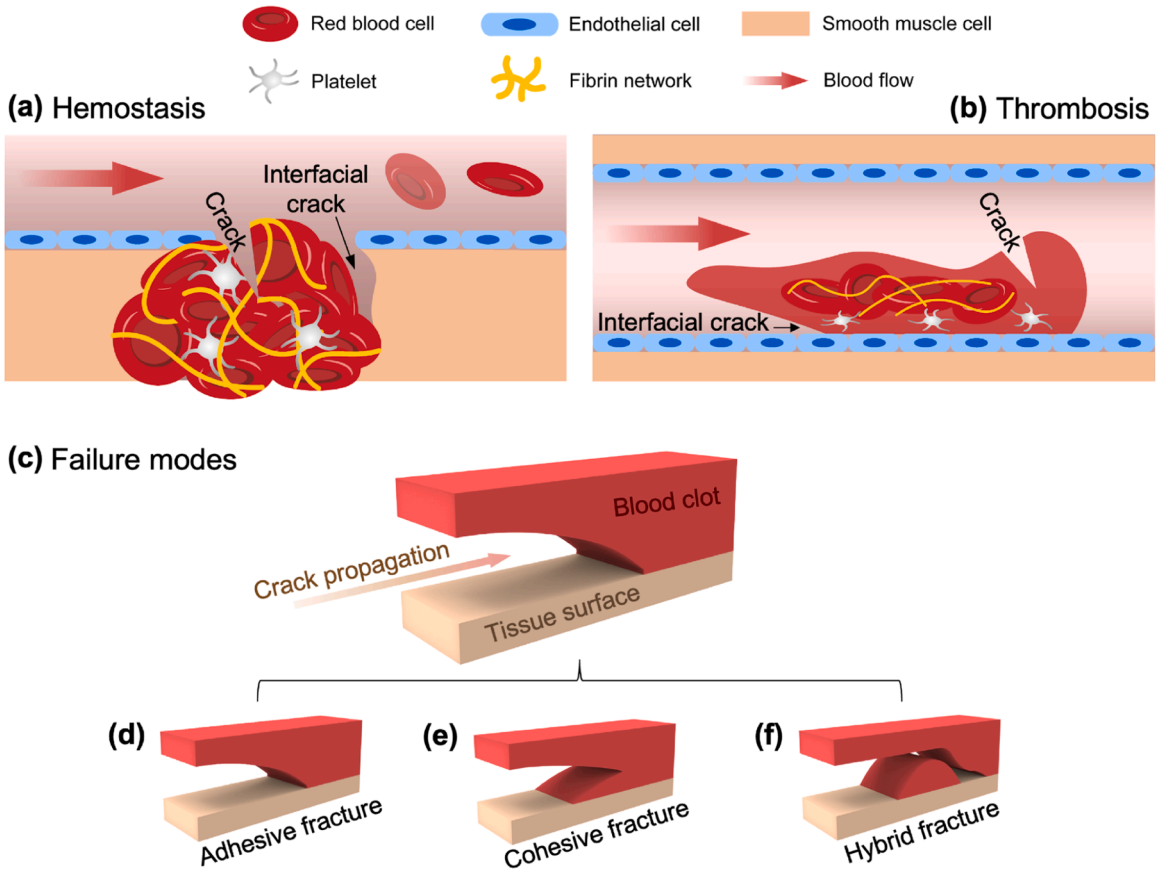

Fig. 1. Schematics of adhesive and cohesive fracture of blood clots. (a-b) Adhesive and cohesive fracture of blood clot in hemostasis (a) and thrombosis (b), led by the propagation of interfacial crack and crack within clots, respectively. (c-f) Different mechanical failure modes of blood clots on biological tissue surfaces, including adhesive fracture (d), cohesive fracture (e), and their combination—hybrid fracture (f).

one of the materials (cohesive). This case of hybrid fracture depends on the interplay between the clot's bulk and adhesion properties to the tissue substrate.

Incorporating adhesive and cohesive fracture in the study of clot fracture presents a holistic framework for understanding the fracture mechanics of clots. To quantify the resistance of clots against fracture, fracture mechanics approaches have been deployed in recent studies, where the bulk fracture energy of blood clots, i.e., the energy required for a unit area of crack growth solely within one material (cohesive fracture) (Mostovoy and Ripling, 1966), was measured using edge-notched and lap-shear tests (Fereidoonnezhad et al., 2021; Liu et al., 2021; Tutwiler et al., 2020). For adhesive fracture, a similar quantity, interfacial adhesion energy, can be used to define the energy required to create a unit area of an interfacial crack (He et al., 1995; Lau et al., 2014). These two properties are correlated, as the interfacial adhesion energy of a material is linked with the energy dissipation within the bulk material, a key contributor to the bulk fracture energy (Gent, 1996). The full picture of clot fracture is yet to be revealed, necessitating a comprehensive investigation to study both the adhesive and cohesive fracture of blood clots.

In this study, we employ an integrated experimental-computational approach to evaluate comprehensively both adhesive and cohesive fracture of blood clots. We performed peeling tests on various substrates (such as muscle, skin, and artery) and pure shear tests to characterize interfacial and bulk fracture energy, respectively. To study the effects of mechanical and cellular factors on clot fracture, we vary the loading rate and the content of RBCs and platelets, and examine the failure mode under different conditions. Furthermore, we build finite element models to capture the mechanical and fracture behaviors of blood clots. These models are parameterized with our experimental results and used to estimate the range of the intrinsic work of fracture and cohesive zone strength for the cohesive zone model formulation. This comprehensive framework lays the groundwork for the assessment and modeling of adhesive and cohesive fracture behavior of blood clots.

2. Methodology

2.1. Blood preparation and clot formation

Bovine whole blood (CPDA-1 anti-coagulant; sourced from McGill Veterinary Services, or Lampire Biological Laboratories, USA) was utilized. Clots were formed through the addition of a calcification solution (10:1 volumetric ratio), resulting in a final concentration of 22.5 mM NaCl and 30 mM $CaCl_2$. Due to the time-sensitivity of platelets, for tests involving platelet content variations, a local source (McGill Veterinary Services) was used, and clotting was performed within 4 h of the blood collection. The remaining tests were completed in <72 h from collection to minimize blood aging and maintain mechanical property consistency (Sugerman et al., 2021a, 2021b).

We modified the RBC content of blood (while keeping the contents of fibrinogen and platelet constant) using the protocol below. The whole blood was aliquoted into 15 mL centrifuge tubes and centrifuged at 1500 g for 15 min. After centrifuging, RBC content settled on the bottom of tubes. The supernatant liquid separated from RBCs is platelet-rich plasma, which contains most of fibrinogen and platelets. Then the supernatant was collected as platelet-rich plasma (PRP) using a pipette, while the remaining was collected as erythrocytes (Raditya and Hernaningsih, 2020). PRP was used to prepare clots with no RBC content (0 %), and unmodified whole blood was used to prepare clots with approximately 50 % RBC content. For 30 % volume ratio of RBC content, we mixed RBCs in unprocessed PRP and normal saline (NS; 0.9% w/v of NaCl) at a volume ratio of 3:5:2 (RBC:PRP:NS) (Zohdi et al., 2010). By leaving a buffer of 0.5 cm above the buffy coat, we carefully pipetted and placed the PRP in a 37 °C incubator, where 40 % of the water was evaporated in approximately 12 h to obtain a concentrated PRP following the protocol modified from a previous study (Mercader Ruiz et al., 2024). RBCs were re-suspended in concentrated PRP (7:3 v:v) to achieve 70 % volume ratio of RBC content blood samples.

We varied platelet contents as follows. The bovine whole blood was centrifuged at 1500 g for 15 min at room temperature to separate PRP and erythrocytes. The PRP was further centrifuged under the same condition. The supernatant which was platelet-poor plasma (PPP) was collected using pipette, and the reminding platelet pellet on the bottom contained most of the platelet content. RBCs were then re-suspended in PPP (1:1 v:v) to create a blood sample devoid of platelets. A blood sample with triple platelet contents was then prepared by mixing the platelet pellet into the zero-platelet blood sample (Dhurat and Sukesh, 2014).

2.2. 90° peeling adhesion tests

To characterize the interfacial adhesion energy of blood clots, we performed 90° peeling tests (Liu et al., 2021; Yang et al., 2021a; Yuk et al., 2016) with various substrates, including bovine muscle, bovine liver, porcine skin, bovine aorta, and gauze (Fig. S1). Rectangular substrates (30 mm x 10 mm x 2 mm) – including bovine muscle, bovine liver, porcine skin, bovine aorta, and gauze – were affixed to a rigid polyethylene terephthalate backing. A silicone mold (Ecoflex 30) with a rectangular chamber (30 mm x 10 mm x 4 mm) was positioned atop the PET plate to enclose the substrate. A scotch tape of 5 mm in length (as a hydrophobic spacer) was applied at the initial part of the substrate to introduce an interfacial crack. Once clotting was started, the blood was pipetted into the chamber, and a flexible backing (polypropylene fabric; 100 mm x 10 mm) was laid on the liquid blood surface with sufficient blood exudation to enhance bonding between the backing and the clot. Samples were incubated at 37 °C for 60 min in humidity bags. Post-incubation, samples were stored at 4 °C overnight and tested the following day. We mounted samples on an Instron machine (model 5965; 10 N loading cell) with a 90° peeling setup and applied vertical displacement on backings at 0.02 mm/s (0.01 s^{-1}), 0.2 mm/s (0.1 s^{-1}) and 2 mm/s (1 s^{-1}; the limit of the testing machine without the inertial effects) loading rates. Strain rates were calculated by dividing the loading rate by the thickness of specimens, which was pre-defined by the height of the space between the backing and substrate (2 mm). The interfacial adhesion energy of the specimen was calculated by (Bao et al., 2022):

$$\Gamma_{adhesion} = P_s / b \tag{1}$$

where P_s is the average peeling force at the plateau, where the peeling force reaches a steady state, and b is the width of peeling specimens.

2.3. Pure shear tests

To measure the bulk fracture energy of blood clots, we performed pure shear tests, which are commonly used to directly measure the fracture energy of soft materials (Long and Hui, 2016). Given the delicate nature of clots, we designed a loading setup for pure shear testing to ensure uniform loading, safe handling, and the creation of wide yet thin samples (40 × 4 × 3 mm) (Fig. S2) (Liu et al., 2024). 3D-printed components were placed on a silicon mold, and a thin polyester film was added to the silicone mold (only for notched samples). After initiating clotting with the recalcification solution, we immediately transferred the blood sample into the pre-assembled pure shear test frame using a pipette. These samples were then incubated at 37 °C for 60 min inside humidity bags to prevent dehydration. Afterward, samples were stored at 4 °C overnight and underwent testing the subsequent day.

The importance of the rate dependency of the interfacial and bulk fracture energy of blood clots is multifaceted. Prior works show that the fracture toughness of clots is sensitive to the loading rate (Liu et al., 2024). This rate dependency reflects how blood clots behave under dynamic physiological loads, such as those experienced during blood flow or muscle contraction. Specifically, the rate-dependent fracture toughness indicates the role of viscoelastic dissipation mechanisms, which contribute to the overall toughness of clots. Understanding this behavior helps in predicting clot stability and potential failure, which is vital for medical applications related to hemostasis and thrombosis.

Both unnotched and notched pure shear samples were used to assess the fracture toughness of clots under different loading rates of 0.04 mm/s (0.01 s^{-1}), 0.4 mm/s (0.1 s^{-1}) and 4 mm/s (1 s^{-1}). The bulk fracture energy was then calculated using the following equation (Long and Hui, 2016):

$$\Gamma_{cohesive} = W(\lambda_c)H_0 \tag{2}$$

where $W(\lambda)$ is the strain energy density in bulk material far ahead of the crack tip and is measured by calculating the area under the stress-strain curve from pure shear tests on unnotched samples. λ_c is the applied stretch ratio at the onset of crack growth, which is measured using the critical fracture strain (where the applied stress reaches its maximum value) of pure shear tests on notched samples. H_0 is the initial height of the sample.

2.4. Scanning electron microscopy

Scanning electron microscopy (SEM) was used to characterize the microstructure of the clot samples subjected to variations in RBC and platelet content, as well as to detect interfacial fracture mode. The microstructure of blood clots was captured using a field emission SEM (F450, FEI). Prior to SEM imaging, all samples underwent sequential ethanol dehydration and hexamethyldisilazane (drying to conserve their original microstructure) (Hazrin-Chong and Manefield, 2012). The dehydrated samples were then coated with 4 nm Pt using a high-resolution sputter coater (ACE600, Leica) to enhance surface conductivity.

2.5. Finite element modeling

To predict the mechanical response of blood clot under unconfined compression and pure shear tests, we used a special compressible Yeoh's strain energy function along with a rate-independent Mullin's damage factor was employed (Ogden and Roxburgh, 1999; Rausch and Humphrey, 2016; Yeoh, 1993):

$$W = \eta W_{\text{dev}} + W_{\text{vol}} + \Phi(\eta) = \eta \sum_{i=1}^{3} C_i(\bar{I}_1 - 3)^i + \frac{1}{D}(J-1)^2 + \Phi(\eta) \tag{3}$$

in which W_{dev} and W_{vol} denote the deviatoric and volumetric free energy function, respectively; Φ is the damage function. The parameters C_1, C_2, C_3 represent hyperelastic material constants of the Yeoh model in a cubic form, D is the material constant for compressible materials, and $\bar{I}_1$ and J are the first deviatoric strain invariant and volumetric change (Ghezelbash et al., 2021; Holzapfel, 2000; Rausch et al., 2021). The damage factor η characterizes the material damage, which equals to 1 for an undeformed material and 0 for fully damaged state, and is determined from the following evolution equation (Ogden and Roxburgh, 1999):

$$\eta = 1 - \frac{1}{r} erf\left(\frac{W_{\text{dev}}^{\max} - W_{\text{dev}}}{m + \beta W_{\text{dev}}^{\max}}\right) \tag{4}$$

where r and m are material constants that characterize the damage properties of a material; β is a positive-value parameter to avoid overly stiff response at the beginning of unloading; erf denotes the error function; and W_{dev}^{max} is the maximum deviatoric strain energy function through the loading history. With η, the damage function $\Phi(\eta)$ takes the following form:

$$\Phi(\eta) = \int_1^{\eta} \left\{ \left(m + \beta W_{\text{dev}}^{\max}\right) erf^{-1}[r(1-\eta)] - W_{\text{dev}}^{\max} \right\} d\eta \tag{5}$$

To determine all material parameters, we minimized the root mean square error between model predictions and experimental data during cyclic loading and compression; see Supplementary Information and Table S1 for additional details.

The cohesive zone model – with a bilinear triangular function – was employed to represent both the midsection of the pure shear samples along the crack plane, as well as the interfacial bonding between the blood clot and tissue (Hui et al., 2011; Tvergaard and Hutchinson, 1993; Wei and Hutchinson, 1998; Yang et al., 2021a). For the bilinear triangular model, the intrinsic work of fracture Γ_0 was defined by utilizing the cohesive zone strength S and the maximum separation δ via $\Gamma_0 = \frac{1}{2}S\delta$. To ensure convergence of peeling simulations, we employed a 4-node linear plane strain quadrilateral element with hourglass control, and modeled the clot-tissue interface by a 4-node two-dimensional cohesive element. For pure shear test simulations, we used 8-node linear brick elements and defined cohesive elements throughout the crack plane in the bulk material. In both simulations, a variety of combinations for intrinsic work of fracture Γ_0 (from 0.5 to 12 J/m^2 with an increment of 0.5) and cohesive zone strength S (from 1 to 8 kPa with an increment of 0.5) was tested. The diagrams were obtained by interpolation using MATLAB between these simulated points.

2.6. Statistical analysis

One-way analysis of variance (ANOVA) was used to compare differences between groups. All data are represented as a mean as well as the standard deviation.

3. Results and discussion

3.1. Interfacial adhesion energy

We quantified adhesive fracture with interfacial adhesion energy (i.e., the energy per unit area needed to detach blood clots from a substrate). The interfacial adhesion energy was measured with 90° peeling tests of blood clots on various substrates, including porcine skin, liver, aorta, muscle and gauze (Fig. 2c). This test has been extensively used to characterize the adhesion of bioadhesives, hydrogels and pressure-sensitive adhesives (Bao et al., 2022; Yang et al., 2021a; Yuk et al., 2016). Fig. 2d shows the representative force per width/displacement curves, where the interfacial adhesion energy was extracted from the nearly plateau regions. Among the tested substrates, we found that the strongest adhesion occurred with gauze, reaching an interfacial adhesion energy of 8.22 ± 0.88 J/m^2. On tissue substrates, interfacial adhesion energy on muscle reached 5.63 ± 2.01 J/m^2, while the weakest adhesion was with inner aorta (1.35 ± 0.39 J/m^2), and liver (2.59 ± 0.89 J/m^2) (Fig. 2e).

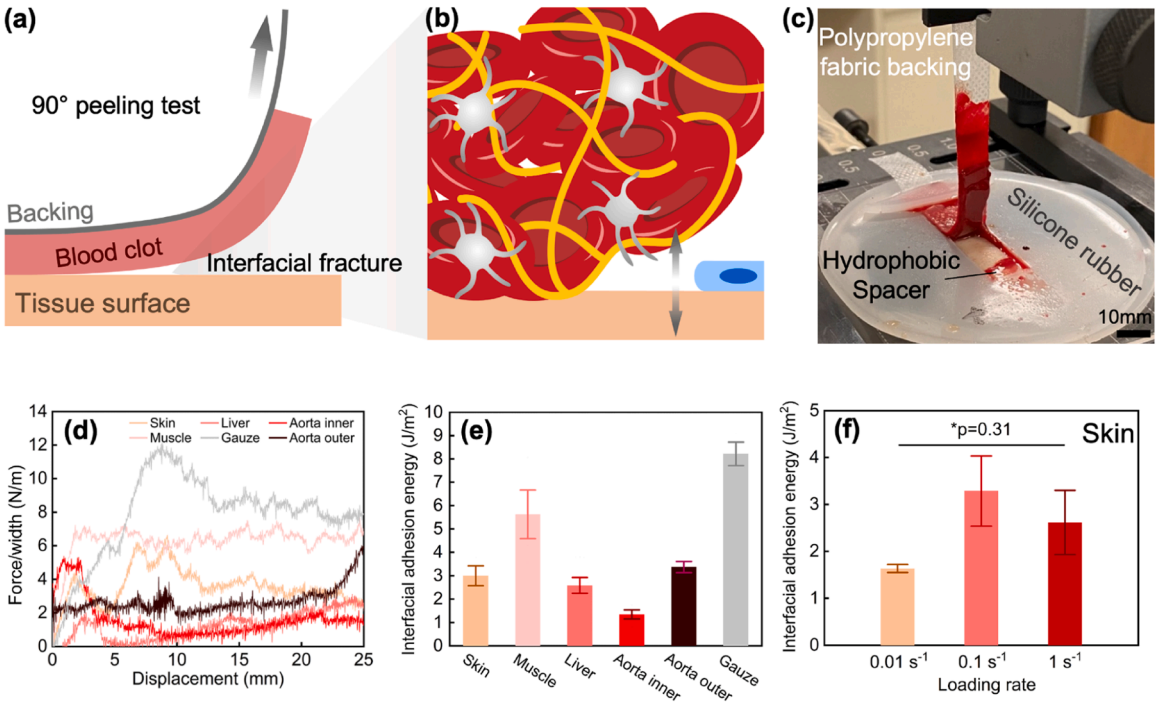

Fig. 2. Characterization of adhesive fracture of blood clots. (a) 90° peeling test of blood clots from a tissue substrate. (b) Crack propagation at the interface between the tissue and the clot, comprising a network of fibrin fibers (yellow), red blood cells and activated platelets. (c) Digital photo of the experimental setup. (d) Representative peeling force/width-displacement curves of blood clots on various substrates. (e) Interfacial adhesion energy of blood clots measured on various substrates (mean ± SD, $n = 4$). (f) Effect of loading rate on interfacial adhesion energy of blood clots on skin (mean ± SD, $n = 4$).

Considering the viscoelastic nature of blood clots, we also investigated how their adhesion performance depends on the peeling rate. We varied the loading rate from 0.01 to 1 s^{-1} due to the limitations of the displacement rate of the Instron machine. As anticipated, the interfacial adhesion energy between the clot and the skin is rate-dependent (Fig. 2f). However, despite a two-order magnitude change in loading rate, the increase of interfacial adhesion energy is less than twofold. This non-monotonic rate dependence of interfacial adhesion energy suggests a distinct rate-dependence of interfacial bonding between the clot and the tissue, in contrast to the bulk fracture and viscoelastic behaviour of bulk clots.

To examine the effect of sample width on our measurements, we further conducted a series of 90-degree peeling tests of different sample widths and compared their measured adhesion energies. The comparison results show that the measured adhesion energy is irrelevant to the sample width; therefore, we believe this testing method could measure the adhesion energy of blood clots as a material property (Fig. S3).

Our measurements indicate that among biological substrates, the blood clot had the strongest adhesion to the muscle tissue and the weakest adhesion to the inner arterial lining (Fig. 2), a phenomenon that harmonizes with the biological role of blood clots. That is, the natural evolution process ensures that blood minimally adheres to the interior walls of blood vessels, facilitating blood flow and mitigating clot formation. This is achieved through the production of anti-adhesive molecules such as heparan sulfate, prostacyclin, and nitric oxide by the endothelial cells within blood vessels, thereby inhibiting blood cells from adhering to the vessel walls (Kohli et al., 2022). Conversely, in muscle injury sites, in addition to the exposure of tissue factors, the exposed collagen fibers in the vessel wall attract and activate platelets to form clots. This attraction is mediated by the von Willebrand factor acting as a bridge, while platelets can also bind directly to collagen via integrin α2β1 and GPVI receptors (Kohli et al., 2022). These factors contribute to the positive correlation between the platelet content and the adhesion performance.

3.2. Bulk fracture energy

We next performed pure shear tests to characterize the cohesive fracture behavior of bovine blood clots (Fig. 3a). Both unnotched and notched specimens were prepared with a customized loading jig and tested with an Instron machine (Fig. 3b and 3c). We measured the bulk fracture energy at 18.27±1.45 J/m^2 under a loading rate of 0.01 s^{-1}. Note that the value is around one order of magnitude larger than the interfacial adhesion energy of the clots measured on skin at the same loading rate. The bulk fracture energy exhibits no sensitivity to variations in the notch length (Fig. 3d), consistent with previous reports (Liu et al., 2021; Tutwiler et al., 2020).

When varying the loading rate, we observed a strong rate dependency in the stress-stretch curves (Fig. 3e). The clots appear stiffer and stronger at higher loading rates. While the failure stretches remain similar, there is a marked increase in the fracture toughness (Fig. 3f). Specifically, the bulk fracture energy increases from 18.27 J/m^2 to 38.12 J/m^2, when the loading accelerated from 0.01 s^{-1} to

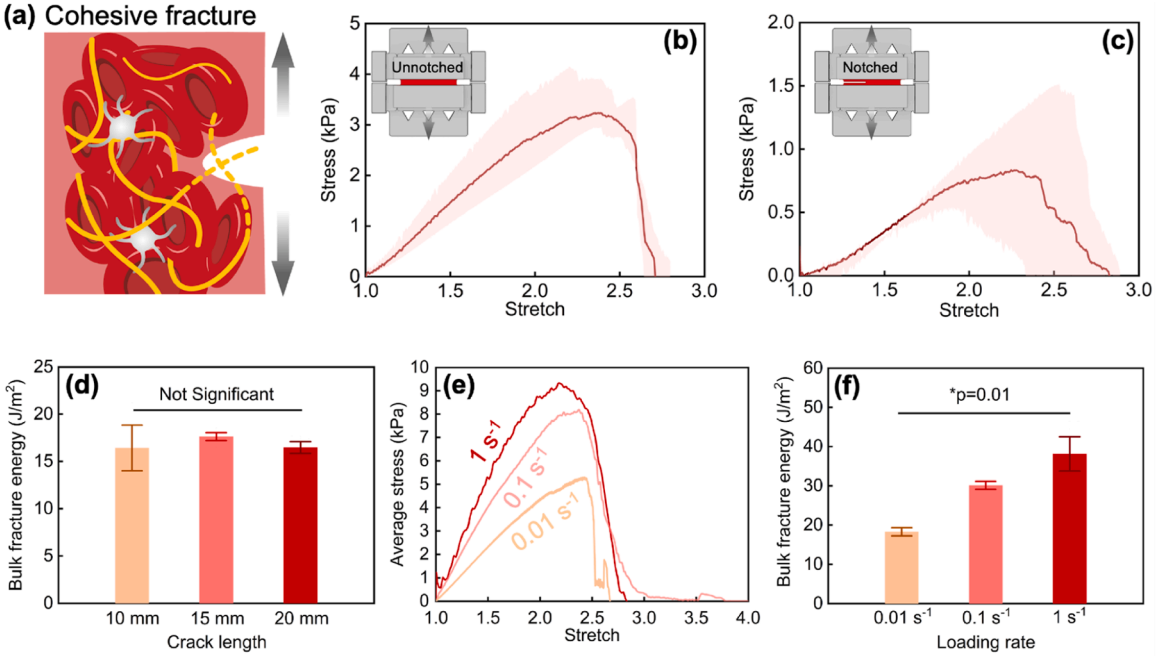

Fig. 3. Characterization of cohesive fracture. (a) Schematic illustration of crack growth within the bulk of blood clots. Average stress-stretch curves of (b) unnotched and (c) notched specimens in pure shear tests (shaded area represents the experimental range; $n = 4$). (d) Bulk fracture energy of blood clots is insensitive to crack length (mean ± SD, $n = 4$). (e) Average stress-stretch curves of unnotched specimens under different loading rates ($n = 4$). (f) Bulk fracture energy of blood clots under different loading rates (mean ± SD, $n = 4$). For statistical analyses, one-way ANOVA was carried out.

$1\ s^{-1}$.

Our results demonstrated that the clot has a strong rate-dependent response (Fig. 2 and 3). Bulk fracture energy within the bulk material exhibited a consistent increase with an increasing loading rate ($0.01\ s^{-1}$ and $1\ s^{-1}$ loading rate); Fig. 2. On the other hand, interfacial adhesion energy showed a rather different trend; while an increase in interfacial adhesion energy was observed at lower loading rates (from $0.01\ s^{-1}$ to $0.1\ s^{-1}$), the effect appeared to be small at larger rates ($>0.1\ s^{-1}$) (Fig. 3). These time-dependent responses can be partly attributed to the poro-visco-elastic nature of the clot. In our mechanical tests, the poro-elastic time constant ($\tau_p = D^2/4Ek$, where τ_p is the time constant, D is the characteristic length for fluid diffusion defined by the sample thickness due to the sample geometry, and E and k represent the elastic modulus and permeability (Ghezelbash et al., 2022)) was estimated at 1 to 3 s, and given the applied loading rates, fluid had sufficient time to exit the tissue. The effect of poro-elasticity on fibrin clot fracture was estimated at a maximum of 15 % (Garyfallogiannis et al., 2023); therefore, the observed rate effects on bulk fracture energy are primarily due to the viscoelasticity of the fibrin network. As the loading rate increases, the fibrin network's viscoelastic response becomes more dominant, resulting in a more resilient clot structure due to increased inter-fibrin interactions and strain-hardening. Recently, the rate-dependent fracture toughness of bovine fibrin clots was reported in another work from our lab (Liu et al., 2024). It has been demonstrated that the viscoelastic dissipation governs the toughening of fibrin clots in our previous study using the same setup and loading rates. When the loading rate was increased from 0.01 /s to 1/s, the fracture toughness of both protein fibrin clots and whole blood clots increased approximately two folds, suggesting similar rate dependence. As expected, the value of fibrin clot toughness is much lower than that of whole blood clots measured here, presumingly due to the contribution from cellular components such as platelets and RBC.

For bovine blood clots, the measured bulk fracture energy ($18.3 \pm 1.5\ J/m^2$) from pure shear tests was larger than the earlier measured values from lap shear ($6.5\ J/m^2$) and edge notch ($8\ J/m^2$; ovine blood) tests (Fereidoonnezhad et al., 2021). Such differences could be in part due to the difference in testing setup and fracture mode. As blood clots are extremely delicate, we designed a customized jig to test the blood clot with minimum handling, manipulation, and processing to maintain clot's structural integrity. Furthermore, we found that a crack length greater than 10 mm does not affect the fracture toughness, since this was much larger than the fracto-sensitive length of the clot (the ratio of the fracture toughness to the work to rupture $\xi = \Gamma / W_*$, estimated at $= 5.3\ mm \pm 0.5$ mm based on the experimental results from this work).

3.3. Effect of RBCs

Despite the high volume fraction (>40 %) of RBC within clots, their mechanical contribution to clot fracture remains unclear. To investigate this, we repeated the mechanical tests with blood clots of varying RBC content. The RBC volume ratio was varied between 0 %, 30 %, 50 %, and 70 % to encompass the range found in different clotting and disease conditions (Folsom et al., 2020). This variation was achieved by concentrating platelet-rich plasma and reconstituting it with RBCs and normal saline (Fig. 4a). We confirmed the differing RBC content in the clots using SEM images (Fig. 4b). In this test, the clots were formed on porcine muscle, followed by 90° peeling tests to determine the interfacial adhesion energy as a function of RBC content. The muscle substrate was selected because it formed the strongest adhesion to clots (Fig. 2e) and is often exposed to clots during bleeding. Additionally, we conducted pure-shear tests to measure the bulk fracture energy of clots with varying RBC content.

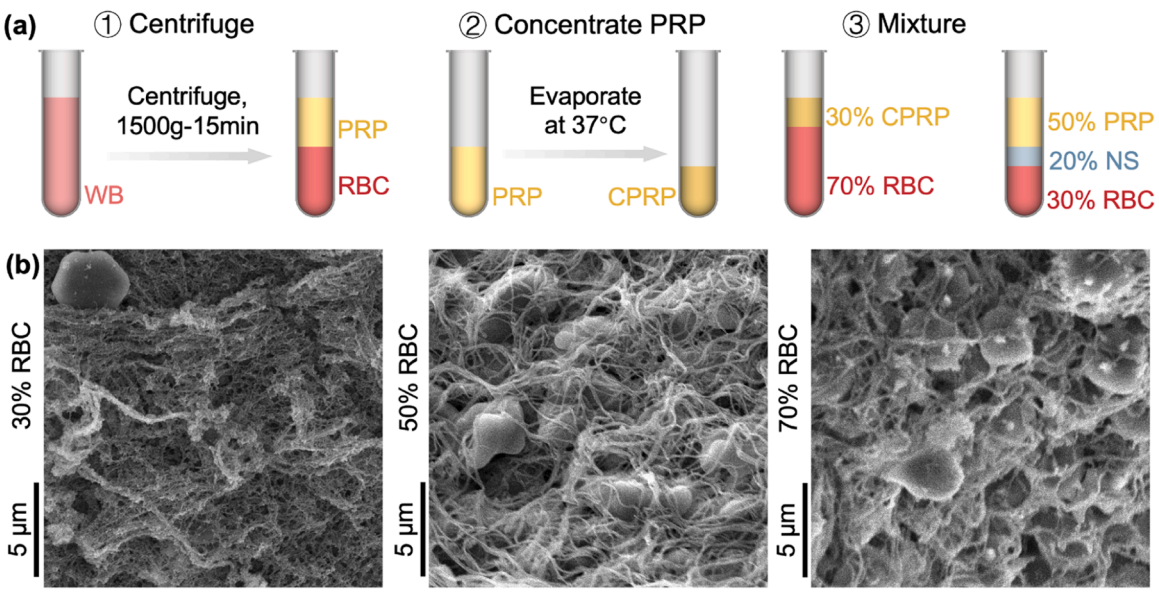

Fig. 4. Blood clots with varying RBC content. (a) Schematic illustrations of preparation process of blood clots with varying RBC content (WB: whole blood; PRP: platelet-rich plasma; RBC: red blood cell; CPRP: concentrated platelet-rich plasma; NS: normal saline). (b) SEM images of blood clots with varying RBC contents (0 %, 30 %, 50 %, and 70 %).

Although RBCs present few functional groups for bioadhesion, their presence significantly impacts both the adhesion and fracture of blood clots. In terms of adhesion between the clot and the muscle, the effect of RBCs is pronounced when the volume ratio is very high. Specifically, a 70 % volume ratio results in an 80 % increase in the interfacial adhesion energy compared to lower volume ratio conditions (Fig. 5a and 5b). Fig. 5c shows the representative stress-stretch curves from pure shear tests. Interestingly, we found that the elastic modulus remains relatively insensitive to RBC content, as the crosslinking of fibrin network dominates the small-strain response (Fig. 5d). This point is supported by the SEM images, showing no notable differences in the fibrin network (Fig. 4b). Notably, increased RBC content raises the critical stretch (Fig. 5e) and thereby the bulk fracture energy (Fig. 5f). Altogether, our findings indicate a synchronized effect of RBCs on both the adhesion and fracture behaviors of clots, with both the interfacial and bulk fracture energies increasing proportionately with RBC content. This phenomenon differs from the dependence on platelet content, as discussed below.

3.4. *Effect of platelets*

We also studied the effect of platelets on the adhesion and fracture of blood clots. Although platelets are present at a much lower volume fraction than RBCs within clots, they provide, if activated, binding with fibrin networks and adhesion to surrounding tissues. Platelets also drive the contraction process through the generation of contractile forces. These forces are propagated through the platelet-fibrin network, which compacts the clot and reduces its volume (Tutwiler et al., 2016), thus playing a more significant mechanical role. In this test, in addition to the condition of physiological platelet concentration (1x), we either depleted or tripled the platelets by centrifugation and re-mixing (Fig. 6a). SEM images confirm the formation of fibrin fiber network, enclosing blood cells (Fig. S4). We then conducted peeling tests and pure-shear tests to characterize adhesive and cohesive fracture of clots with varying platelet content.

For the peeling tests, we first examined the cracked surface of the post-mortem specimens, showing the specimens of elevated platelet content (3x) displayed a hybrid fracture (i.e., combined adhesive and cohesive fracture). Visual inspection and SEM images revealed residual fibrin fibers and blood cells on the muscle substrate (Fig. 6b). In contrast, the specimens of normal platelet content (1x) showed negligible traces of clot residue on the muscle substrate, indicative of an adhesive fracture (Fig. 6b). Consistent with the fracture model transition, we found that the interfacial adhesion energy increased with the platelet content (Fig. 7a-b). Pure shear tests further confirmed the mechanical significance of platelets in terms of the bulk mechanical properties. Fig. 7c shows the stress-stretch curves of unnotched specimens of varying platelet content. Interestingly, the measured elastic moduli showed no significant difference (Fig. 7d). However, increased platelet contents substantially reduced the critical stretch of notched specimens (Fig. 7e), so as the bulk fracture energy (Fig. 7f). These findings underscore the critical role of platelets in determining the adhesion and fracture behavior of blood clots.

The focus of previous studies has been predominantly on cohesive fracture within the bulk clot, yet the interfacial crack propagation, as an independent mechanism of failure, receives much less attention. Consider the blood clot detaches from substrate tissues

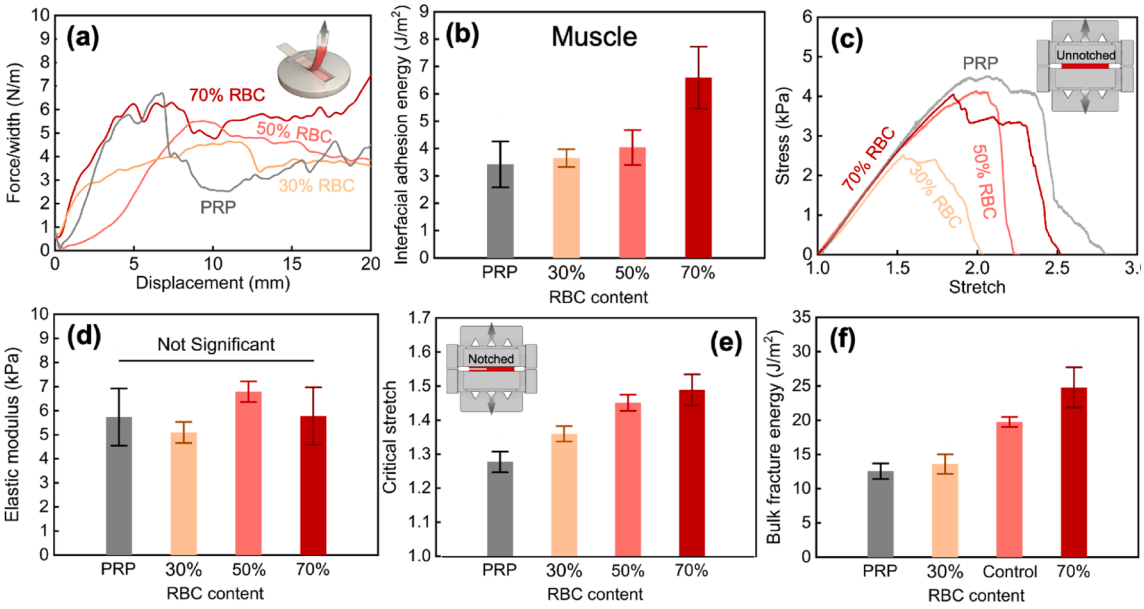

Fig. 5. Effects of RBC on mechanical properties of blood clots. (a) Average load-displacement curves of blood clots for different RBC contents (0 %, 30 %, 50 %, and 70 %) on muscle substrate in 90° peeling tests. (b) Interfacial adhesion energy of blood clots on muscle for different RBC content (mean ± SD, $n = 4$). (c) Average stress-stretch response of the blood clot under pure shear test (unnotched specimens) for different RBC content (mean ± SD, $n = 4$). The effect of RBC content on (d) elastic modulus and (e) critical stretch of the blood clot under pure shear test. (f) Fracture toughness of blood clot for different RBC content measured from pure shear test (mean ± SD, $n = 4$).

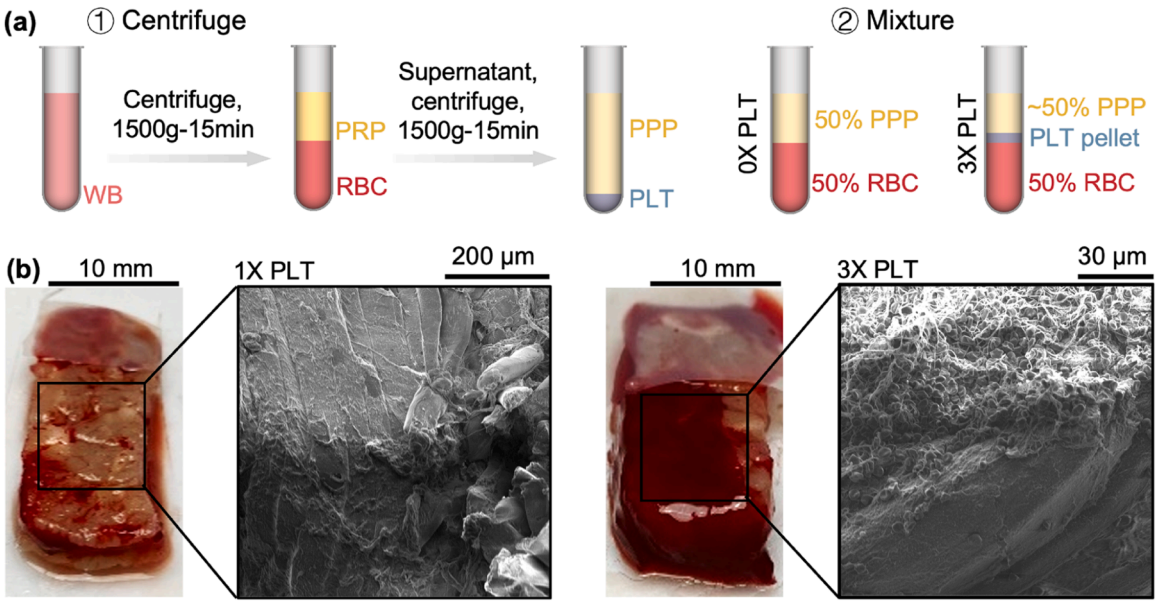

Fig. 6. Blood clots with varying platelet content. (a) Preparation process of blood with different platelet contents (WB: whole blood; PRP: platelet-rich plasma; PPP: platelet-poor plasma; RBC: red blood cell; PLT: platelet). (b) SEM images of blood clots with 1x and 3x PLT after peeling tests showing residues on bovine muscle substrates after peeling test.

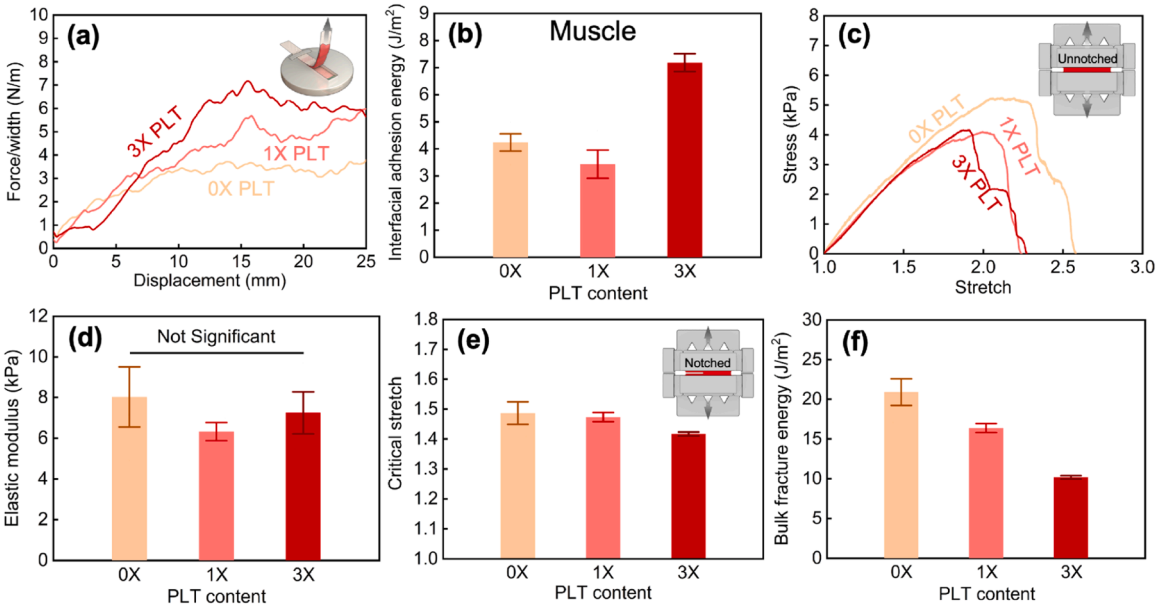

Fig. 7. Effects of platelet content on mechanical properties of blood clots. (c) Average force/width-displacement curves of blood clots (0x, 1x, and 3x PLT) on muscle substrate in 90° peeling tests. (d) Interfacial adhesion energy of blood clots on muscle for different platelet content (mean ± SD, $n = 4$). (e) Average stress-stretch curves of the blood clots under pure shear test (unnotched specimens) for different platelet content (mean ± SD, $n = 4$). The effect of PLT content on (f) elastic modulus and (g) critical stretch of blood clots under pure shear test. (h) Bulk fracture energy of blood clots as a function of platelet content (mean ± SD, $n = 4$).

(such as skin or arteries), and through this process adhesive, cohesive, and hybrid fracture can take place (Fig. 1). In comparison to fracture toughness within the bulk material (Fig. 3), we measured much lower interfacial adhesion energy across all tested biological tissues (Fig. 2), suggesting a higher likelihood for adhesive fracture. This observation underscores that the adhesion property is a key limiting factor for blood clot fracture, especially under the context of hemostasis involving the contact between the clot and surrounding tissues. Our peeling tests further confirmed the predominance of adhesive fracture, with SEM imaging revealing only small

residuals of the blood clot left on the substrate tissue (Fig. 6b). The fracture mode was shifted to be a hybrid mode when the platelet content increased 3x from the normal level. It is worth noting that we characterized interfacial and bulk fracture energies using different tests (peeling and pure shear), and a direct comparison of these values should be practiced with caution.

3.5. Finite element model

We built two finite element models to simulate the cohesive and adhesive fracture of blood clots, respectively, using a coupled cohesive-zone and Mullins-effect model validated by our experiments. Although blood clots exhibit significant rate dependence, we chose to focus on their rate-independent mechanical responses for this initial model development. Given that the clots display hyperelastic and Mullin's responses, we combined the Yeoh model and the Mullins model, both calibrated with experimental data from cyclic loading and compression tests. In the peeling simulation, the substrate was modeled as porcine skin (Yang et al., 2021a). The parameters used are listed in Table S2 and S3. Both the Yeoh and Mullins models are phenomenological, using empirical data and mathematical formulations to describe material behavior without explaining the underlying microstructures. Fig. 8a shows a good agreement between the simulated and experimental data obtained from unnotched pure-shear specimens under cyclic tensile loading (Fig. 8a). Similar agreement was observed in the unidirectional compression tests (Fig. 8b). Furthermore, the constitutive model, paired with the cohesive zone model discussed below, can reasonably well capture the stress-stretch curve of the notched pure-shear specimens up to the rupture point (Fig. 8c).

The cohesive zone model was used to simulate the fracture within the bulk and at the interface between the clot and porcine skin. For the skin substrate, we used the Ogden model developed before (Yang et al., 2021a). The cohesive zone model defines the traction-separation law for crack propagation. In the form of bilinear triangular function, it involves the intrinsic work of fracture Γ_0, cohesive zone strength S and the maximum separation δ_c. Determining these exact values is technically challenging, so we conducted a parameter study by screening various combinations for intrinsic work of fracture Γ_0 and cohesive zone strength S. With them, the traction-separation law was defined and the FEM could output bulk fracture energy for the pure-shear model and interfacial adhesion energy for the peeling model. Fig. 8d illustrates the simulated fracture energy as function of Γ_0 and S, and the adhesion energy diagram is shown in Fig. 8e. Using these two diagrams, we considered the fracture and adhesion energies measured at the lowest loading rates to

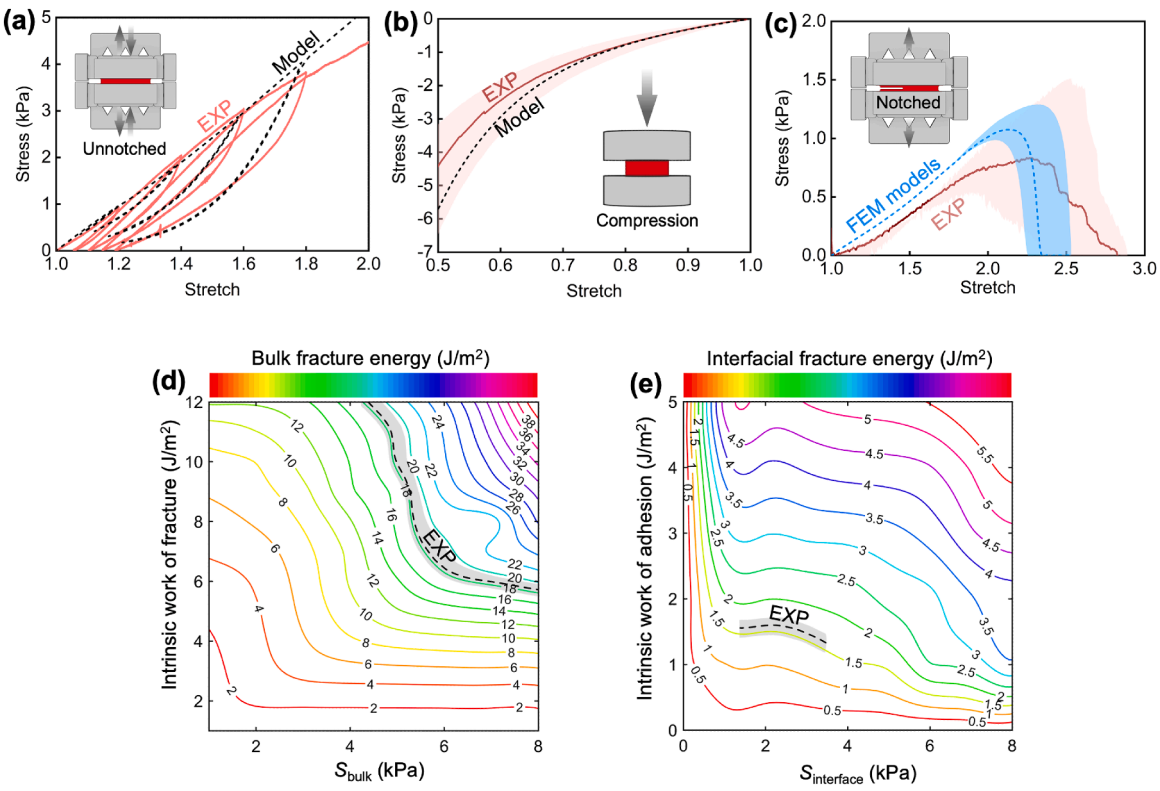

Fig. 8. Finite element modelling of blood clots. (a-b) Stress-stretch curves of blood clots under pure shear cyclic loading (a) and unconfined compression tests (b) obtained from our experiments (red) and finite element models (black). (c) Stress-stretch curves of the notched blood clot specimen under pure shear tests obtained from experiments (red) and finite element models (blue). (d) Simulated bulk fracture energy of the blood clot for various cohesive zone model parameters (intrinsic work of fracture: Γ_0^{bul}; cohesive zone strength for bulk fracture: S_{bulk}). The black dot line indicates the average experiment result. (e) Simulated interfacial adhesion energy of the blood clot for various cohesive zone model parameters (intrinsic work of adhesion: Γ_0^{int}; cohesive zone strength for interfacial fracture: $S_{interface}$). The black dot line indicates the average experiment result.

minimize the rate-dependent contributions. The counter lines indicate the range of Γ_0 and S could allow the model to yield the bulk fracture and interfacial adhesion energies consistent with experimental results, whilst satisfying the criteria for Γ_0 and the typical strain concentration factors observed for blood clots.

This cohesive zone model has widespread application in engineered and soft materials, including hydrogels and bioadhesives (Yang et al., 2021a, 2021b; Yuk et al., 2016; Zhang et al., 2017). Within the framework, one needs to identify two parameters: the intrinsic work of fracture Γ_0 and the cohesive zone strength S. Both parameters are difficult to determine experimentally. However, recent efforts have attempted to determine the intrinsic work of fracture through fatigue fracture tests, specifically by determining the fatigue threshold below which no crack propagation under cyclic loading. For instance, another paper from our group reports the fatigue threshold of bovine fibrin clots (i.e., blood cell-free plasma clot) measured at 1.66 J/m^2 (Liu et al., 2024). Yet, conducting such tests presents technical challenges due to the extended testing duration required, especially incompatible with whole blood clots containing various blood cells and sensitive biological components.

To further confine the range, we account for the physical range of Γ_0 and S. Specifically, Γ_0 cannot exceed the experimentally measured fracture energy. For S, its value cannot fall below the bulk strength (~4 kPa) observed in pure shear tests and the peeling strength (~1.7 kPa) during peeling, and the maximum value of S can be approximately estimated as its minimum value multiplied by the strain concentration factor at crack tip (Tang et al., 2024; Tutwiler et al., 2021, 2020). These considerations lead to that S is likely lower than 8 kPa in cohesive fracture and 3.5 kPa in adhesive fracture. For instance, by adhering to the constraint of S and matching the simulation and experimentally measured fracture energy under the lowest loading rate (~18.3 J/m^2), when observing S_{bulk} exceeding 5.2 kPa in some experimental results, we could identify a suitable range for Γ_0^{bul} between 6 and 8 J/m^2 (Fig. 8d). With the values, our FEM reasonably captured the stress-strain curves of notched specimens under pure shear tests (Fig. 8c). The FEM can reveal the stress, strain, and displacement fields in the clot during cohesive and adhesive fracture, enable the estimation of intrinsic fracture energy and cohesive zone strength that are difficult to measure directly, and further provide valuable insights for understanding and modelling fracture mechanisms of blood clots.

Compared with fibrin clot (blood cell-free plasma clot) (Liu et al., 2024), both the overall bulk fracture toughness and intrinsic fracture toughness of whole blood clots are significantly higher, further indicating the important role of blood cells in the clot toughening. Applying the same methodology above, we estimated a suitable range for Γ_0^{int} between 1.3 and 1.6 J/m^2 with $S_{\text{interface}}$ exceeding 1.7 kPa from the adhesion energy diagram (Fig. 8e). A close examination of the prediction results reveals that the intrinsic work of adhesion is comparable to the interfacial adhesion energy, suggesting minimal bulk energy dissipation in blood clot adhesion, in contrast to cohesive fracture, where the bulk fracture energy significantly exceeds the intrinsic work of fracture. These findings not only enable the development of FEMs to simulate blood clot fracture and adhesion but also offer valuable insights into the underlying fracture mechanisms.

Interfacial adhesion energy arises from both the surface-to-surface bonds between adjacent materials (i.e., intrinsic work of fracture) as well as energy dissipation within the bulk material (Li et al., 2017). Blood clots exhibit strong hysteresis under cyclic loading (Liu et al., 2024), indicating a strong potential for bulk energy dissipation, which in turn toughens adhesion. To corroborate this point, our finite element model for peeling tests reveals that eliminating bulk material dissipation (i.e., simulating an elastic response devoid of the Mullin effect) reduces the interfacial adhesion energy by 31 %, underscoring the coupling between interfacial and bulk mechanical characteristics. This indicates that understanding and controlling the adhesion of blood clots should involve not only interfacial properties but also bulk material properties.

4. General discussion

Using an integrated experimental-computational methodology, we studied the adhesive/cohesive fracture mechanics of bovine blood clots, and evaluated the effects of loading rates and cellular components (RBC and platelet) on the clot fracture mechanics. Upon examination of the results, we found that the interfacial adhesion energy is significantly smaller than the bulk fracture energy in all loading rates tested. While both increase with the loading rate, the rate dependence of the bulk fracture energy is more potent than that of interfacial adhesion energy. Our results also reveal the mechanical contribution of RBC and platelets to the adhesion/cohesive fracture of blood clots, which is further rationalized with the characterization of bulk mechanical properties. A picture of biological cell-modulating clot fracture emerges: the increasing RBC content toughens the clots against both cohesive and adhesive fracture, while the platelet content raises interfacial adhesion energy and eventually shifts the fracture mode from adhesive to hybrid fracture. With the characterized mechanical and fracture properties of blood clots, we built a finite element model, successfully capturing the rate-independent multi-modal behavior of the blood clot. This study provides novel insights into the fracture mechanics of blood clots and brings valuable implications to the biomedical applications associated with blood clots and thrombosis. Below are some general discussions of this study.

4.1. Cell-mediated mechanical properties

Unlike polymer chains, the impact of biological cells on fracture is unexplored. While the mechanical role of platelets in blood clots has been widely recognized (Lam et al., 2011; Tutwiler et al., 2017; Wufsus et al., 2013, 2015), RBC is traditionally underappreciated mechanically. RBCs primarily affect clots in vivo by influencing rheological behaviors, including laminar shearing, platelet margination, aggregation, and RBC deformability. RBCs directly interact with fibrin, impacting the structure, mechanical properties, and lytic resistance of clots and thrombi. Furthermore, studies on clot contraction reveal that contracted clots form an impermeable and

compacted barrier composed of polyhedral-shaped RBCs (Litvinov and Weisel, 2017).

This study reveals the significant contribution of biological cells to the fracture properties of blood clots, but the elastic modulus of blood clots is insensitive to the content of RBCs and platelets. Given the softness of RBC, they do not affect the elastic modulus measured at small strains, which is mainly governed by the fibrin network. The weak dependence of elastic modulus on the platelet content is noteworthy. We attribute this phenomenon to the fact that our pure-shear specimens could not contract due to the constraints of the clotting mold, and clot contraction is the key mechanism of platelet-driven clot stiffening. Furthermore, the clot contraction was found to require a high threshold value of platelet content, below which the elastic modulus of blood clots mainly depends on the fibrin content (Boodt et al., 2021). This effect was confirmed with our experiment of blood clots with or without a myosin inhibitor (blebbistatin), showing pre-strain measured at 11 %−15 % (Fig. S5).

Our results clearly demonstrate that increased RBC content enhances both interfacial and bulk fracture energies. We interpret this effect as follows. Fracture energy has generally two contributors: the intrinsic fracture toughness derived from bond breaking at the crack tip (Γ_{in}) and the energy dissipation contribution from the bulk matrix (Γ_D). The RBC could influence the energy dissipation process in the process zone within the bulk matrix. Another possibility is that the presence of RBC could influence the configuration of fibrin fibers and their crosslinking network (Gersh et al., 2009), which have effects on both Γ_{in} and Γ_D. There are several crosslinking mechanisms of blood clots, including fibrin crosslinking, cell-cell adhesion and cell-fibrin binding (Jiang et al., 2022). Further investigation is warranted to pinpoint the underlying mechanism of RBC-mediated fracture.

We found different effects of RBCs and platelets on the mechanical properties of clots and attributed these differences to their polymer binding capacity. Platelets participate in secondary hemostasis, influencing fibrin network formation and crosslinking. The contribution of platelets to clot adhesion has been documented (Chan et al., 2020; Eriksson and Whiss, 2005; Qiu et al., 2014). Our experiments demonstrate a significant enhancement in interfacial adhesion energy by a factor of two with higher platelet counts (Fig. 7b). The adhesion mechanism of platelets is discussed as follows. Platelet adhesion and activation occur upon exposure to collagen and tissue factor-bearing cells at the injury site (Davie et al., 1991). Activated platelets bind collagen fibers via fibrinogen-mediated interplay with platelet surface integrins, forming a platelet plug to stop hemorrhage (Govindarajan et al., 2018). Also, the exposed collagen and immobilized von Willebrand factor further interact with platelets through platelet membrane receptors, leading to platelet adhesion.

In contrast to the positive effect on adhesion, increased platelet content tends to embrittle the fibrin network, resulting in reduced bulk fracture toughness—a contrast to the consistent reinforcement observed with RBCs. We attribute this effect to platelet contraction facilitated by contractile elements like actin and myosin, inducing prestress in the clots (Sun et al., 2022). Although additional platelets are often believed to improve structural integrity (Darcourt et al., 2021), their potential benefit appears counterbalanced by the contraction-induced reduction in bulk fracture energy. The effect of platelets is so profound that it shifted the mechanical failure mode seen in our peeling tests—from predominantly adhesive fracture to hybrid fracture within the specimens with increased platelet content.

4.2. Clinical implications

Understanding the mechanics of blood clots, including the distinct roles of adhesive and cohesive fracture in clot failure and the impact of RBC and platelet contents, has important clinical implications. Consider the application of wound management. An ideal wound dressing should balance its adhesion to the tissue and clot; it should attach firmly to the surrounding tissue to efficiently stop bleeding yet maintain minimal adhesion to the clot itself to avoid disruption and potential re-bleeding upon removal. However, gauze – the most common wound dressing material – seems to contradict this notion. In a skin injury, the gauze has almost zero adhesion to the skin, rendering it unable to adequately seal the wound site. Meanwhile, our peeling tests have shown that gauze exhibits the highest adhesion to the clot (Fig. 2). This elevated clot adherence can lead to cohesive fracture within the clot during dressing removal, triggering a re-bleeding event, a situation familiar to many healthcare practitioners and patients.

4.3. Limitations

This study has several limitations. The blood clots tested here were formed under static conditions *in vitro*, which differ from physiological conditions *in vivo*. Despite these differences, thrombin-induced clots from bovine blood have demonstrated mechanical properties similar to those of human blood clots formed in arteries (Chueh et al., 2011). It is worth noting that using in vivo-formed human clots for this study was not feasible due to restrictions related to sample size and technical considerations. Also, blood clots formed in vivo exhibit significant variability, particularly in their cellular components. For example, the composition and formation of venous and arterial thrombi differ due to various physiological, pathological and treatment conditions, which could lead to substantial changes in their mechanical properties. Therefore, we prepared in vitro blood clots to minimize its variance and ensure consistency in mechanical testing. Future research should be done to examine the correlation between in vitro and in vivo formed clots.

Another limitation is the delay associated with shipping time, typically around 24 h, which is expected to render some platelets in the blood source inactive, which could influence the results (Egidi et al., 2010; Josefsson et al., 2014). Lastly, our finite element modeling was rate-independent and also did not account for the viscoelastic effect, but given that we were examining a single rate, this assumption remained adequate for our study's purposes. As the blood clots exhibit viscoplastic behavior, the effect of permanent deformation or plasticity is worth consideration in future investigations (Fereidoonnezhad and McGarry, 2022; Ghezelbash et al., 2022; van Kempen et al., 2016).

5. Conclusion

This study revealed the pivotal roles of loading rate and biological cells in the adhesion and fracture of blood clots. The interfacial adhesion energy also increased with the loading rate, though this effect diminished at high loading rate. In comparison, the bulk fracture energy was significantly larger, while exhibiting more pronounced rate dependency. The clots exhibited the highest adhesion to gauze (larger than other biological substrates) and paradoxically failed to adhere to the skin to seal the wound efficiently, risking disruption and potential re-bleeding upon gauze removal. An increase in RBC content amplified both interfacial adhesion and bulk fracture energies, with adhesive fracture emerging as the dominant fracture mode. Additionally, higher platelet content enhanced interfacial adhesion energy to the point where the failure mode in peeling tests shifted from adhesive to hybrid fracture, underscoring the crucial role of platelets in adhesion. We also developed a finite element model that captured the complex loading-unloading blood clot behavior in various loading and fracture conditions, including cyclic loading, compression, cohesive fracture under pure shear tests and adhesive fracture during peeling. This model enabled us to estimate the intrinsic work of fracture and the cohesive zone strength for blood clot fracture. These findings significantly enhance our understanding of clot mechanics, with important clinical implications for optimizing the management of clot-related disorders and paving the way for the development of innovative, more efficient wound dressings.

CRediT authorship contribution statement

Shiyu Liu: Writing – review & editing, Writing – original draft, Visualization, Validation, Software, Resources, Methodology, Investigation, Formal analysis, Data curation. **Aram Bahmani:** Writing – review & editing, Visualization, Software, Investigation. **Gabriella Paige Sugerman:** Investigation, Data curation. **Zhen Yang:** Methodology, Investigation. **Manuel Rausch:** Investigation, Data curation. **Farshid Ghezelbash:** Writing – original draft, Supervision, Methodology, Investigation, Conceptualization. **Jianyu Li:** Writing – review & editing, Supervision, Project administration, Funding acquisition, Conceptualization.

Declaration of competing interest

The authors declare that they have no known competing financial interests or personal relationships that could have appeared to influence the work reported in this paper.

Data availability

Data will be made available on request.

Acknowledgment

This study was supported by the Canadian Institutes of Health Research (grant PJT-180232, J.L.). S.L. and A.B. were financially supported by a McGill Engineering Doctoral Award (MEDA). J.L. acknowledges the support from Canada Research Chairs Program and International Excellence Fellowship from Karlsruhe Institute of Technology. M.K. acknowledges support by the National Science Foundation through grants 2235856, 2127925, 2105175, 2046148 and the Office of Naval Research under grant N00014-23-2575.

Supplementary materials

Supplementary material associated with this article can be found, in the online version, at doi:10.1016/j.jmps.2024.105858.

References

Ackermann, M., Verleden, S.E., Kuehnel, M., Haverich, A., Welte, T., Laenger, F., Vanstapel, A., Werlein, C., Stark, H., Tzankov, A., Li, W.W., Li, V.W., Mentzer, S.J., Jonigk, D., 2020. Pulmonary vascular endothelialitis, thrombosis, and angiogenesis in Covid-19. N. Engl. J. Med. 383, 120–128. https://doi.org/10.1056/nejmoa2015432.

Bao, G., Gao, Q., Cau, M., Ali-Mohamad, N., Strong, M., Jiang, S., Yang, Z., Valiei, A., Ma, Z., Amabili, M., Gao, Z.-H., Mongeau, L., Kastrup, C., Li, J., 2022. Liquid-infused microstructured bioadhesives halt non-compressible hemorrhage. Nat. Commun. 13 https://doi.org/10.1038/s41467-022-32803-1.

Bayer, I.S., 2022. Advances in fibrin-based materials in wound repair: a review. Molecules 27, 4504. https://doi.org/10.3390/molecules27144504.

Boodt, N., Snouckaert Van Schauburg, P.R.W., Hund, H.M., Fereidoonnezhad, B., McGarry, J.P., Akyildiz, A.C., Van Es, A.C.G.M., De Meyer, S.F., Dippel, D.W.J., Lingsma, H.F., Van Beusekom, H.M.M., Van Der Lugt, A., Gijsen, F.J.H., 2021. Mechanical characterization of thrombi retrieved with endovascular thrombectomy in patients with acute ischemic stroke. Stroke 52, 2510–2517. https://doi.org/10.1161/strokeaha.120.033527.

Brown, A.C., Barker, T.H., 2014. Fibrin-based biomaterials: modulation of macroscopic properties through rational design at the molecular level. Acta Biomater 10, 1502–1514. https://doi.org/10.1016/j.actbio.2013.09.008.

Chan, K.Y.T., Yong, A.S.M., Wang, X., Ringgold, K.M., St John, A.E., Baylis, J.R., White, N.J., Kastrup, C.J., 2020. The adhesion of clots in wounds contributes to hemostasis and can be enhanced by coagulation factor XIII. Sci. Rep. 10, 20116. https://doi.org/10.1038/s41598-020-76782-z.

Chueh, J.Y., Wakhloo, A.K., Hendricks, G.H., Silva, C.F., Weaver, J.P., Gounis, M.J., 2011. Mechanical characterization of thromboemboli in acute ischemic stroke and laboratory embolus analogs. Am. J. Neuroradiol. 32, 1237–1244. https://doi.org/10.3174/ajnr.a2485.

Darcourt, J., Demchuk, A.M., Olivot, J.-M., 2021. Platelets and clot stiffness: a challenge but also an opportunity toward achieving consistent complete reperfusion. Stroke 52, 2518–2520. https://doi.org/10.1161/strokeaha.121.035105.
Davie, E.W., Fujikawa, K., Kisiel, W., 1991. The coagulation cascade: initiation, maintenance, and regulation. Biochemistry 30, 10363–10370. https://doi.org/10.1021/bi00107a001.
Dhurat, R., Sukesh, M., 2014. Principles and methods of preparation of platelet-rich plasma: a review and author's perspective. J. Cutan. Aesthet. Surg. 7, 189–197. https://doi.org/10.4103/0974-2077.150734.
Egidi, M.G., D'Alessandro, A., Mandarello, G., Zolla, L., 2010. Troubleshooting in platelet storage temperature and new perspectives through proteomics. Blood Transfus 8 (3), s73–s81. https://doi.org/10.2450/2010.012s. Suppl.
Eriksson, A.C., Whiss, P.A., 2005. Measurement of adhesion of human platelets in plasma to protein surfaces in microplates. J. Pharmacol. Toxicol. Methods 52, 356–365. https://doi.org/10.1016/j.vascn.2005.06.002.
Fereidoonnezhad, B., Dwivedi, A., Johnson, S., McCarthy, R., McGarry, P., 2021. Blood clot fracture properties are dependent on red blood cell and fibrin content. Acta Biomater 127, 213–228. https://doi.org/10.1016/j.actbio.2021.03.052.
Fereidoonnezhad, B., McGarry, P., 2022. A new constitutive model for permanent deformation of blood clots with application to simulation of aspiration thrombectomy. J. Biomech. 130, 110865 https://doi.org/10.1016/j.jbiomech.2021.110865.
Folsom, A.R., Wang, W., Parikh, R., Lutsey, P.L., Beckman, J.D., Cushman, M., 2020. Hematocrit and incidence of venous thromboembolism. Res. Pract. Thromb. Haemost. 4, 422–428. https://doi.org/10.1002/rth2.12325.
Garyfallogiannis, K., Ramanujam, R.K., Litvinov, R.I., Yu, T., Nagaswami, C., Bassani, J.L., Weisel, J.W., Purohit, P.K., Tutwiler, V., 2023. Fracture toughness of fibrin gels as a function of protein volume fraction: mechanical origins. Acta Biomater 159, 49–62. https://doi.org/10.1016/j.actbio.2022.12.028.
Gent, A.N., 1996. Adhesion and strength of viscoelastic solids. Is there a relationship between adhesion and bulk properties? Langmuir 12, 4492–4496. https://doi.org/10.1021/la950887q.
Gersh, K.C., Nagaswami, C., Weisel, J.W., 2009. Fibrin network structure and clot mechanical properties are altered by incorporation of erythrocytes. Thromb. Haemost. 102, 1169–1175. https://doi.org/10.1160/TH09-03-0199.
Ghezelbash, F., Eskandari, A.H., Shirazi-Adl, A., Kazempour, M., Tavakoli, J., Baghani, M., Costi, J.J., 2021. Modeling of human intervertebral disc annulus fibrosus with complex multi-fiber networks. Acta Biomater 123, 208–221. https://doi.org/10.1016/j.actbio.2020.12.062.
Ghezelbash, F., Liu, S., Shirazi-Adl, A., Li, J., 2022. Blood clot behaves as a poro-visco-elastic material. J. Mech. Behav. Biomed. Mater. 105101 https://doi.org/10.1016/j.jmbbm.2022.105101.
Govindarajan, V., Zhu, S., Li, R., Lu, Y., Diamond, S.L., Reifman, J., Mitrophanov, A.Y., 2018. Impact of tissue factor localization on blood clot structure and resistance under venous shear. Biophys. J. 114, 978–991. https://doi.org/10.1016/j.bpj.2017.12.034.
Hazrin-Chong, N.H., Manefield, M., 2012. An alternative SEM drying method using hexamethyldisilazane (HMDS) for microbial cell attachment studies on sub-bituminous coal. J. Microbiol. Methods 90, 96–99. https://doi.org/10.1016/j.mimet.2012.04.014.
He, M.Y., Turner, M.R., Evans, A.G., 1995. Analysis of the double cleavage drilled compression specimen for interface fracture energy measurements over a range of mode mixities. Acta Metall. Mater. 43, 3453–3458. https://doi.org/10.1016/0956-7151(95)00036-U.
Holzapfel, G.A., 2000. Nonlinear Solid mechanics: A continuum Approach For Engineering. Wiley Chichester, Chichester.
Hui, C.Y., Ruina, A., Long, R., Jagota, A., 2011. Cohesive zone models and fracture. J. Adhes. 87, 1–52. https://doi.org/10.1080/00218464.2011.538315.
Jiang, S., Liu, S., Lau, S., Li, J., 2022. Hemostatic biomaterials to halt non-compressible hemorrhage. J. Mater. Chem. B 10, 7239–7259. https://doi.org/10.1039/d2tb00546h.
Jiang, Y., Liang, X., Guo, M., Cao, Y., Cai, S., 2018. Fracture mechanics modeling of popping event during daughter cell separation. Biomech. Model. Mechanobiol. 17, 1131–1137. https://doi.org/10.1007/s10237-018-1019-6.
Josefsson, E.C., Burnett, D.L., Lebois, M., Debrincat, M.A., White, M.J., Henley, K.J., Lane, R.M., Moujalled, D., Preston, S.P., O'Reilly, L.A., Pellegrini, M., Metcalf, D., Strasser, A., Kile, B.T., 2014. Platelet production proceeds independently of the intrinsic and extrinsic apoptosis pathways. Nat. Commun. 5 https://doi.org/10.1038/ncomms4455.
Kohli, S., Shahzad, K., Jouppila, A., Holthöfer, H., Isermann, B., Lassila, R., 2022. Thrombosis and inflammation—A dynamic interplay and the role of glycosaminoglycans and activated protein C. Front. Cardiovasc. Med. 9 https://doi.org/10.3389/fcvm.2022.866751.
Lam, W.A., Chaudhuri, O., Crow, A., Webster, K.D., Li, T.-D., Kita, A., Huang, J., Fletcher, D.A., 2011. Mechanics and contraction dynamics of single platelets and implications for clot stiffening. Nat. Mater. 10, 61–66. https://doi.org/10.1038/nmat2903.
Lau, D., Broderick, K., Buehler, M.J., Büyüköztürk, O., 2014. A robust nanoscale experimental quantification of fracture energy in a bilayer material system. PNAS 111, 11990–11995. https://doi.org/10.1073/pnas.1402893111.
Laurens, N., Koolwijk, P., De Maat, M.P.M., 2006. Fibrin structure and wound healing. J. Thromb. Haemost. 4, 932–939. https://doi.org/10.1111/j.1538-7836.2006.01861.x.
Li, J., Celiz, A.D., Yang, J., Yang, Q., Wamala, I., Whyte, W., Seo, B.R., Vasilyev, N.V., Vlassak, J.J., Suo, Z., Mooney, D.J., 2017. Tough adhesives for diverse wet surfaces. Science 357, 378–381. https://doi.org/10.1126/science.aah6362.
Litvinov, R.I., Weisel, J.W., 2017. Role of red blood cells in haemostasis and thrombosis. ISBT Sci. Ser. 12, 176–183.
Litvinov, R.I., Weisel, J.W., 2022. Blood clot contraction: mechanisms, pathophysiology, and disease. Res. Pract. Thromb. Haemost. 100023 https://doi.org/10.1016/j.rpth.2022.100023.
Liu, S., Bahmani, A., Ghezelbash, F., Li, J., 2024. Fibrin clot fracture under cyclic fatigue and variable rate loading. Acta Biomater 177, 265–277. https://doi.org/10.1016/j.actbio.2024.01.046.
Liu, S., Bao, G., Ma, Z., Kastrup, C.J., Li, J., 2021. Fracture mechanics of blood clots: measurements of toughness and critical length scales. Extreme Mech. Lett. 48, 101444 https://doi.org/10.1016/j.eml.2021.101444.
Long, R., Hui, C.-Y., 2016. Fracture toughness of hydrogels: measurement and interpretation. Soft Matter 12, 8069–8086. https://doi.org/10.1039/c6sm01694d.
Mercader Ruiz, J., Beitia, M., Delgado, D., Sánchez, P., Sánchez, M.B., Oraa, J., Benito-Lopez, F., Basabe-Desmonts, L., Sánchez, M., 2024. Method to obtain a plasma rich in platelet- and plasma-growth factors based on water evaporation. PLoS ONE 19, e0297001. https://doi.org/10.1371/journal.pone.0297001.
Mostovoy, S., Ripling, E.J., 1966. Fracture toughness of an epoxy system. J. Appl. Polym. Sci. 10, 1351–1371. https://doi.org/10.1002/app.1966.070100913.
Ogden, R.W., Roxburgh, D.G., 1999. A pseudo–elastic model for the Mullins effect in filled rubber. Proc. R. Soc. A: Math. Phys. Eng. Sci. 455, 2861–2877. https://doi.org/10.1098/rspa.1999.0431.
Qiu, Y., Brown, A.C., Myers, D.R., Sakurai, Y., Mannino, R.G., Tran, R., Ahn, B., Hardy, E.T., Kee, M.F., Kumar, S., Bao, G., Barker, T.H., Lam, W.A., 2014. Platelet mechanosensing of substrate stiffness during clot formation mediates adhesion, spreading, and activation. PNAS 111, 14430–14435. https://doi.org/10.1073/pnas.1322917111.
Qiu, Y., Myers, D.R., Lam, W.A., 2019. The biophysics and mechanics of blood from a materials perspective. Nat. Rev. Mater. 4, 294–311. https://doi.org/10.1038/s41578-019-0099-y.
Raditya, P.P.R., Hernaningsih, Y., 2020. Platelet counts analysis of platelet-poor plasma (PPP) produced by several centrifugation techniques. Indian J. Med. Forensic Med. Toxicol. 14 https://doi.org/10.37506/ijfmt.v14i3.10559.
Rausch, M.K., Humphrey, J.D., 2016. A microstructurally inspired damage model for early venous thrombus. J. Mech. Behav. Biomed. Mater. 55, 12–20. https://doi.org/10.1016/j.jmbbm.2015.10.006.
Rausch, M.K., Sugerman, G.P., Kakaletsis, S., Dortdivanlioglu, B., 2021. Hyper-viscoelastic damage modeling of whole blood clot under large deformation. Biomech. Model. Mechanobiol. 1–13. https://doi.org/10.1007/s10237-021-01467-z.
Sugerman, G.P., Chokshi, A., Rausch, M.K., 2021a. Preparation and mounting of whole blood clot samples for mechanical testing. Curr. Protoc. 1 https://doi.org/10.1002/cpz1.197.
Sugerman, G.P., Kakaletsis, S., Thakkar, P., Chokshi, A., Parekh, S.H., Rausch, M.K., 2021b. A whole blood thrombus mimic: constitutive behavior under simple shear. J. Mech. Behav. Biomed. Mater. 115, 104216 https://doi.org/10.1016/j.jmbbm.2020.104216.

Sugerman, G.P., Parekh, S.H., Rausch, M.K., 2020. Nonlinear, dissipative phenomena in whole blood clot mechanics. Soft Matter 16, 9908–9916. https://doi.org/10.1039/d0sm01317j.
Sun, Y., Oshinowo, O., Myers, D.R., Lam, W.A., Alexeev, A., 2022. Resolving the missing link between single platelet force and clot contractile force. iScience 25, 103690. https://doi.org/10.1016/j.isci.2021.103690.
Tanaka, K.A., Key, N.S., Levy, J.H., 2009. Blood coagulation: hemostasis and thrombin regulation. Anesth. Analg. 108 https://doi.org/10.1213/ane.0b013e31819bcc9c.
Tang, J., Lin, J., Wang, T., 2024. Cracking of soft collagenous tissues under suture retention. J. Mech. Phys. Solids 105682. https://doi.org/10.1016/j.jmps.2024.105682.
Tutwiler, V., Litvinov, R.I., Lozhkin, A.P., Peshkova, A.D., Lebedeva, T., Ataullakhanov, F.I., Spiller, K.L., Cines, D.B., Weisel, J.W., 2016. Kinetics and mechanics of clot contraction are governed by the molecular and cellular composition of the blood. Blood 127, 149–159. https://doi.org/10.1182/blood-2015-05-647560.
Tutwiler, V., Maksudov, F., Litvinov, R.I., Weisel, J.W., Barsegov, V., 2021. Strength and deformability of fibrin clots: biomechanics, thermodynamics, and mechanisms of rupture. Acta Biomater 131, 355–369. https://doi.org/10.1016/j.actbio.2021.06.046.
Tutwiler, V., Singh, J., Litvinov, R.I., Bassani, J.L., Purohit, P.K., Weisel, J.W., 2020. Rupture of blood clots: mechanics and pathophysiology. Sci. Adv. 6, eabc0496. https://doi.org/10.1126/sciadv.abc0496.
Tutwiler, V., Wang, H., Litvinov, R.I., Weisel, J.W., Shenoy, V.B., 2017. Interplay of platelet contractility and elasticity of fibrin/erythrocytes in blood clot retraction. Biophys. J. 112, 714–723. https://doi.org/10.1016/j.bpj.2017.01.005.
Tvergaard, V., Hutchinson, J.W., 1993. The influence of plasticity on mixed mode interface toughness. J. Mech. Phys. Solids 41, 1119–1135. https://doi.org/10.1016/0022-5096(93)90057-M.
van Kempen, T.H., Donders, W.P., van de Vosse, F.N., Peters, G.W., 2016. A constitutive model for developing blood clots with various compositions and their nonlinear viscoelastic behavior. Biomech. Model. Mechanobiol. 15, 279–291. https://doi.org/10.1007/s10237-015-0686-9.
Wei, Y., Hutchinson, J.W., 1998. Interface strength, work of adhesion and plasticity in the peel test. Int. J. Fract. 93, 315–333. https://doi.org/10.1023/a:1007545200315.
Wufsus, A.R., Macera, N.E., Neeves, K.B., 2013. The hydraulic permeability of blood clots as a function of fibrin and platelet density. Biophys. J. 104, 1812–1823. https://doi.org/10.1016/j.bpj.2013.02.055.
Wufsus, A.R., Rana, K., Brown, A., Dorgan, J.R., Liberatore, M.W., Neeves, K.B., 2015. Elastic behavior and platelet retraction in low- and high-density fibrin gels. Biophys. J. 108, 173–183. https://doi.org/10.1016/j.bpj.2014.11.007.
Yang, Z., Ma, Z., Liu, S., Li, J., 2021a. Tissue adhesion with tough hydrogels: experiments and modeling. Mech. Mater. 157, 103800 https://doi.org/10.1016/j.mechmat.2021.103800.
Yang, Z., Zhu, Z., Xia, Y., Yang, F., Sun, Y., Jiang, H., 2021b. Modified cohesive zone model for soft adhesive layer considering rate dependence of intrinsic fracture energy. Eng. Fract. Mech. 258, 108089 https://doi.org/10.1016/j.engfracmech.2021.108089.
Yeoh, O.H., 1993. Some forms of the strain energy function for rubber. Rubber Chem. Technol. 66, 754–771. https://doi.org/10.5254/1.3538343.
Yuk, H., Zhang, T., Lin, S., Parada, G.A., Zhao, X., 2016. Tough bonding of hydrogels to diverse non-porous surfaces. Nat. Mater. 15, 190–196. https://doi.org/10.1038/nmat4463.
Zhang, T., Yuk, H., Lin, S., Parada, G.A., Zhao, X., 2017. Tough and tunable adhesion of hydrogels: experiments and models. Acta Mech. Sin. 33, 543–554. https://doi.org/10.1007/s10409-017-0661-z.
Zohdi, T.I., Kuypers, F.A., Lee, W.C., 2010. Estimation of red blood cell volume fraction from overall permittivity measurements. Int. J. Eng. Sci. 48, 1681–1691. https://doi.org/10.1016/j.ijengsci.2010.04.013.